IEEE Access
Multidisciplinary | Rapid Review | Open Access Journal

Received June 13, 2019, accepted June 29, 2019, date of publication July 8, 2019, date of current version July 24, 2019.

Digital Object Identifier 10.1109/ACCESS.2019.2927264

An Efficient Volumetric SBR Method for Electromagnetic Scattering From In-Homogeneous Plasma Sheath

ZHOU CONG, ZI HE, (Member, IEEE), AND RUSHAN CHEN, (Senior Member, IEEE)
Department of Communication Engineering, Nanjing University of Science and Technology, Nanjing 210094, China

Corresponding author: Zi He (15850554055@163.com)

This work was supported in part by the Natural Science Foundation of China under Grant 61890540, Grant 61890541, Grant 61431006, Grant 61771246, and Grant 61701232, in part by the Jiangsu Province Natural Science Foundation under Grant BKs20170854, in part by the Young Elite Scientists Sponsorship Program by the CAST under Grant 2017QNRC001, and in part by the China Postdoctoral Science Foundation under Grant 2017M620861 and Grant 2018T110127.

ABSTRACT A novel volumetric shooting and bouncing ray (VSBR) method is first proposed to analyze the electromagnetic scattering from in-homogeneous plasma sheath. The propagation of electromagnetic waves in a plasma sheath can be accurately traced by using rays in volumetric-meshed cells. The algorithm starts with tracking the ray tubes in the plasma sheath with high efficiency. Then, the reflection and transmission coefficients can be obtained by using the theory of electromagnetic waves' propagation in the lossy medium. At last, the scattering far fields can be easily calculated by taking the scattering field of each tube into consideration. As a comparison, the state-of-the-art high-frequency algorithms cannot deal with in-homogeneous lossy mediums of rapid varying. Meanwhile, it should also be noted that the proposed method can provide a more accurate result for analyzing layered plasma sheath than traditional high-frequency methods. Moreover, in this paper, the cubes' model with a different dielectric parameter, blunt cone, and hyper-sonic models are calculated with the finite-difference time-domain method (FDTD), the volume-surface integral equation method (VSIE), the traditional high-frequency method, and the proposed method. The results demonstrate the accuracy and efficiency of the proposed method.

INDEX TERMS Inhomogeneous plasma, shooting and bouncing ray, tetrahedron, plasma sheath.

I. INTRODUCTION

The electromagnetic scattering analysis of the plasma sheath has attracted increasing attention in recent years. It has a significant effect on vehicle identification, recognition, signal communication and flight control. The interaction between the electromagnetic wave and plasma includes reflecting, refracting and absorbing, which will influence the radar detection. As a result, it will lead to the black barrier phenomenon since the energy of the electromagnetic wave decays in the plasma sheath.

In the last decades, a lot of research has been done to obtain the EM characteristics of the plasma sheath object. The electromagnetic scattering characteristics of the plasma sheath is firstly calculated by the Born approximation method [1]. Studies were then mainly concerned with the frequency of the L and S bands. In 1992, Gregoire *et al*. used the Wentzel-Kramers-Brillouin (WKB) method to analyze the collision and absorption characteristics of the EM wave in the plasma sheath [2]. Subsequent to this, the EM wave propagation properties in a moving non-uniform plasma were studied by combining WKB methods and relativistic effects [3]. In 2001, Shi*et al* used a numerical method to consider the electromagnetic reflection problem of a conductive plane covered by magnetized non-uniform plasma, where the plasma electron density distribution is assumed to be a parabola [4]. Then some new numerical methods have been proposed to analyze the scattering from plasma sheath, in which the fluid dynamic equation is used to obtain the flow fields. In 2007, Yuan and Shi calculated EM scattering by plasma spheres with a plasma layer with Drude model adopted [5]. In 2009, Bhaskar*et al.* studied the radar cross section of a flat plate covered with cold colliding non-uniform plasma [6]. Lately, a numerical procedure for the analysis of

The associate editor coordinating the review of this manuscript and approving it for publication was Ying Liu.

electromagnetic scattering by a hyper-sonic cone-like body flying in the near space was presented [7]. Also, some studies of solving the Navier-Stokes equation to resolve the flow fields were done with modified WKB method [8] and Born approximate method [9]. In addition, Guo et al. have investigated the influence of the electromagnetic wave's scattering characteristics on the dusty plasma by using JE convolution-finite-difference time-domain (JEC-FDTD) method [10].

However, the computation consumption of rigorous numerical methods is insufferable for electrically large targets.

Therefore, the development of high-frequency methods has a great significance. In recent years, the physical optics (PO) formulations and generalized reflection coefficient theory have been derived for conductive objects with in-homogeneous plasma coverage. It can be used as an efficient tool to analyze the arbitrarily layered plasma [11]. However, it will have a bad performance for in-homogeneous plasma whose medium changes rapidly varying positions.

In this paper, the new shooting and bouncing ray method (VSBR) based on the tetrahedral meshing is presented to analyze the plasma sheath targets. Considering the propagation inside the in-homogeneous plasma mediums, the electromagnetic waves are tracing by ray tubes. With the application of fluid field simulation software (CFD-FASTRON), the fluid field distribution of the in-homogeneous plasma around the vehicle is achieved. By using the Debye model, the equivalent permittivity of each plasma cell is calculated. It should be noted that the permittivity is mapped to each tetrahedron cell. In this way, the equivalent permittivity of the in-homogeneous medium target can be accurately modeled. At last, the contribution of all rays through the medium body are considered to get the scattering field. Numerical results are given to validate the accuracy and efficiency of the proposed method.

II. VOLUMETRIC PLASMA SHEATH MODEL

In this section, a plasma sheath model based on tetrahedral meshing is established. As the tetrahedral cells are small enough, each cells can be approximated as a uniform medium in the entire non-uniform plasma sheath region. The whole process is shown in Fig 1 (e).

A. TETRAHEDRAL CELLS IN PLASMA SHEATH

As shown in Fig 1 (a) and (b), the plasma sheath is tetrahedral meshed to obtain a large number of separate uniform lossy medium cells. The interfaces of tetrahedral cells are divided into three cases:

Case 1: The air and medium interfaces. Case 2: The interface between two mediums. Case 3: The interface between the medium and the metal part of the model. The ANSYS software is employed to model and mesh the 3D plasma sheath object. The global scale is usually set to 1/8 of the operating wavelength. It ensures that the mesh of the target can describe its shape. If the size of the tetrahedral cells is too small, the unknowns will increase a lot, thus the calculation time and memory will be improved greatly.

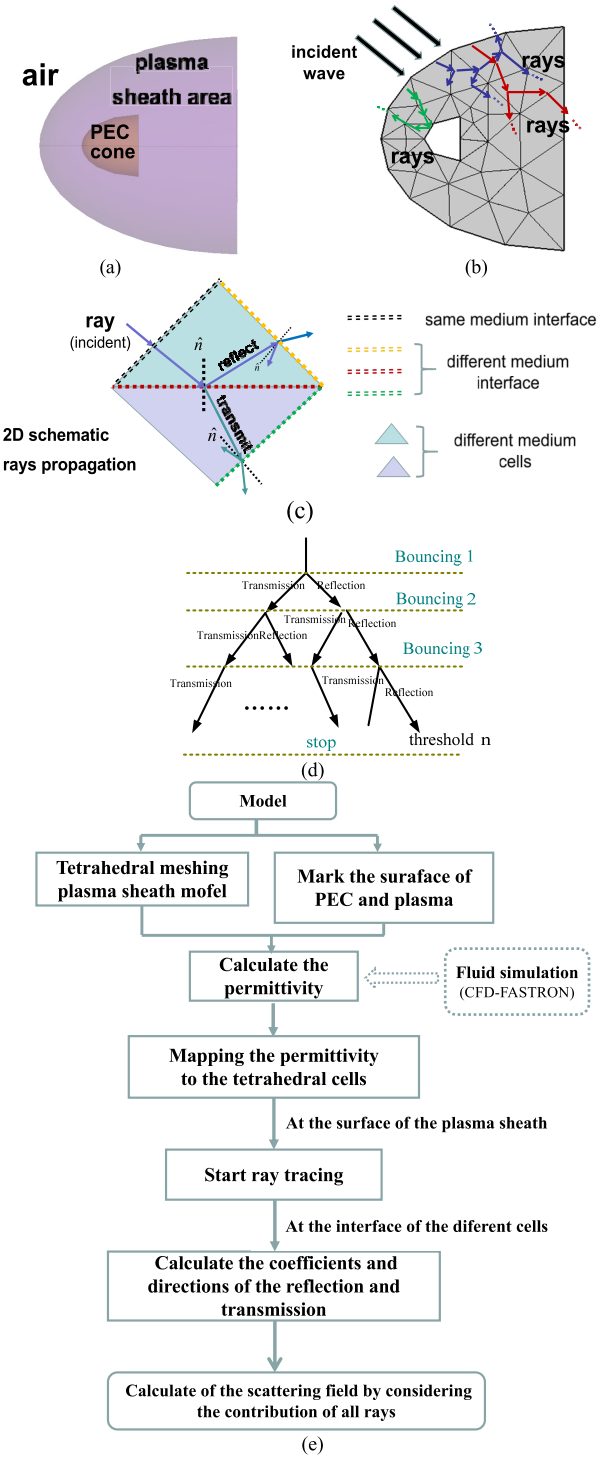

FIGURE 1. (a) Model structure of the plasma sheath. (b) Two-dimensional plan of tetrahedral meshed plasma sheath and the ray tracing way in the tetrahedron cells of object. (c) Reflecting and transmitting of rays at the interface of the different tetrahedral cells with different dielectric constant. (d) Threshold for the number of bounces of the ray. (e) Flow chart of the VSBR method for calculating plasma sheath scattering problems.

B. RAY TRACING IN PLASMA SHEATH

According to the ray tracing method, the outermost discrete triangular facets (Case 1) of the tetrahedron at the target

surface are regarded as discrete initial ray tubes. The rays are directly emitted from the surface of the target. The ray direction of the first reflection and transmission at the target surface are considered as the initial exit direction. Considering the propagation of rays inside the mediums, it is necessary to determine whether reflection and transmission will occur when the rays propagate to the interface of two tetrahedral cells (Case 2). As shown in Fig 1 (c), if the dielectric parameters on both sides of the interface are the same or with little difference, the change of the ray propagation path can be neglected and the wave passes through directly. If the dielectric parameters differ greatly, the direction and electric field of the corresponding reflected and transmitted rays are calculated according to the reflection and transmission rule. Total reflection occurs when a ray incident on the interface between the medium and the metal part (Case 3). As shown in Fig 1(d), the ray will stop transmitting or reflecting after several number of bounces. This threshold number is dependent on the loss of the medium.

C. PLASMA FLOW FIELD SIMULATION

The flow field distribution of the inhomogeneous medium is computed by CFD-FASTRON software [12], [13]. As the condition of the height and Mach flight speed, the CFD-FASTRAN software is divided by hexahedrons and the number of vertices on the hexahedrons equals to the number of unknowns. Each unknown represents the values of temperature and pressure [13]. From the unknowns extracted the electron density n_e and the temperature T, plasma frequency ω_p and collision frequency ν_e can be calculated as follow [8]:

$$\omega_p = 8974\sqrt{n_e}, \quad \nu_e = 5.2 \times 10^{13} \cdot n_e \cdot kk \cdot T \tag{1}$$

Then by using the Debye model, which is a good approximation for steady-state and nu-magnetized plasma [14], the real and imaginary parts of the complex permittivity in each cell can be expressed as:

$$re(\varepsilon_r) = 1 - \frac{\omega_p^2}{\omega^2 + \nu_e^2}, \quad im(\varepsilon_r) = -\frac{\omega_p^2 \cdot \nu_e}{\omega(\omega^2 + \nu_e^2)} \tag{2}$$

Here, n_e is electron density and kk is Boltzmann constant, ω is the incident wave frequency, ω_p is the plasma frequency, ν_e is the collision frequency, ε_r is the equivalent permittivity of the plasma, and the permeability μ_r is 1.0.

D. MAPPING PERMITTIVITY

The ε_r in the hexahedron cells is first to be calculated. Then, the ε_r should be mapped to the tetrahedral cells. Each value of the vertices is mapped to each tetrahedral cells. Then an average value is obtained while mapping the ε_r and μ_r in each tetrahedral cell.

III. WAVE PROPAGATION THROUGH PLASMA SHEATH

The plasma sheath is considered as an aggregation of different lossy mediums. The electromagnetic waves propagating through the interface of different medium will produce reflection and refraction. If each medium is non-consumable, according to Snell's law, the angle of reflection and refraction can be easily obtained. However, as the plasma sheath is a lossy medium, at the interface, the relative permittivity and permeability of the lossy medium are expressed as a complex number. Thus, the traditional law is not relevant to further transmission analysis and the non-uniform plane wave is used to analyzing the lossy medium [15].

A. PROPAGATION OF NON-UNIFORM WAVE

Non-uniform means the directions of constant phase and amplitude planes of the wave are not identical and there is an angle θ ($0 < \theta \leq \pi/2$) between them [16]–[18]. As illustrated in Fig. 2, a non-uniform wave with amplitude vector $\vec{\alpha}_1$ and phase vector $\vec{\beta}_1$ propagate from medium 1 to medium 2 through the interface. $\vec{\alpha}_2$ is the amplitude vector of the transmitted non-uniform wave and $\vec{\beta}_2$ is the phase vector. It is supposed that the incident wave propagation vector is a complex vector $\vec{\gamma}_1 = \vec{\alpha}_1 + j\vec{\beta}_1$. θ_1 is the angle between $\vec{\alpha}_1$ and $\vec{\beta}_1$. When the incident wave pass, the angle between the interface normal vector $\hat{n}$ and phase vector $\vec{\beta}_1$ denoted by φ_1. The angle in medium 2 between the phase vector $\vec{\beta}_2$ and normal vector $\hat{n}$ is φ_2. Meanwhile, the angle between $\vec{\alpha}_2$ and $\vec{\beta}_2$ is θ_2 [15].

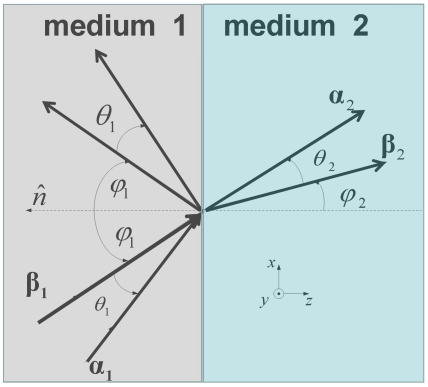

FIGURE 2. The angles and directions to describe the wave propagation at the interface of two different lossy mediums.

According to the Adler–Chu–Fano formulation [16], the propagation vector between medium 1 and medium 2 are expressed as:

$$\vec{\gamma}_i = \alpha_i(\sin\zeta_i\hat{e}_x + \cos\zeta_i\hat{e}_z) + j\beta_i(\sin\varphi_i\hat{e}_x + \cos\varphi_i\hat{e}_z) \tag{3}$$

where i is the medium number and $\zeta_i = \varphi_i + \theta_i$.The relationship between the propagation vector and intrinsic propagation constant γ_{0i} defined above is as:

$$\vec{\gamma}_i \cdot \vec{\gamma}_i = \gamma_{0i} \tag{4}$$

The constant γ_{0i} is only related to the medium characteristic as:

$$\begin{aligned}\gamma_{0i} &= \alpha_{0i} + j\beta_{0i} = jk_0\sqrt{\varepsilon_{ri}\mu_{ri}} \\ &= \frac{\omega}{c}\sqrt{|\varepsilon_{ri}|\,|\mu_{ri}|}\,(\sin\sigma + j\cos\sigma)\end{aligned} \tag{5}$$

while

$$\sigma = \frac{1}{2}\left[\arctan\left(\frac{\varepsilon''_{ri}}{\varepsilon'_{ri}}\right) + \arctan\left(\frac{\mu''_{ri}}{\mu'_{ri}}\right)\right] \tag{6}$$

where the complex relative permittivity and permeability of medium i is $\varepsilon_{ri} = \varepsilon'_{ri} - j\varepsilon''_{ri}$ and $\mu_{ri} = \mu'_{ri} - j\mu''_{ri}$.

By applying equation (4), the equation (7) is obtained as:

$$\alpha_i^2 - \beta_i^2 = \alpha_{0i}^2 - \beta_{0i}^2, \quad \alpha_i\beta_i\cos\rho_i = \alpha_{0i}\beta_{0i} \tag{7}$$

It is assumed that electromagnetic waves are time harmonic electromagnetic waves and the phase is continuous at the interface, If the propagation constant and angle θ_2 in medium 1 is known, the α_1 and β_1 in the propagation vector can be obtained by the equation as:

$$\begin{aligned}\alpha_1 &= \sqrt{\frac{\beta_{01}^2 - \alpha_{01}^2}{2}}\sqrt{\sqrt{1 + (\frac{2\alpha_{01}\beta_{01}}{(\beta_{01}^2 - \alpha_{01}^2)\cos\theta_1})^2} - 1}\\ \beta_1 &= \sqrt{\frac{\beta_{01}^2 - \alpha_{01}^2}{2}}\sqrt{\sqrt{1 + (\frac{2\alpha_{01}\beta_{01}}{(\beta_{01}^2 - \alpha_{01}^2)\cos\theta_1})^2} + 1}\end{aligned} \tag{8}$$

where α_2 and β_2 can be obtained by the equation as:

$$\begin{aligned}\alpha_2 &= \sqrt{\frac{1}{2}(|\gamma_{1t}|^2 + \mathrm{Re}(\gamma_{02}^2) + |\gamma_{1t}^2 - \gamma_{02}^2|)}\\ \beta_2 &= \sqrt{\frac{1}{2}(|\gamma_{1t}|^2 - \mathrm{Re}(\gamma_{02}^2) + |\gamma_{1t}^2 - \gamma_{02}^2|)}\end{aligned} \tag{9}$$

where

$$\begin{aligned}|\gamma_{1t}|^2 &= \alpha_2^2\sin^2\zeta_2 + \beta_2^2\sin^2\varphi_2\\ \mathrm{Re}\left(\gamma_{02}^2\right) &= \alpha_2^2 - \beta_2^2 + 2j\alpha_2\beta_2\cos\theta_2\\ \left|\gamma_{1t}^2 - \gamma_{02}^2\right| &= \alpha_2^2\cos^2\zeta_2 + \beta_2^2\cos^2\varphi_2\end{aligned} \tag{10}$$

in which the α_1, β_1 and α_2, β_2 is solved. Meanwhile, the angle φ_2 and θ_2 in medium 2 can be solved. This expression is suitable for ray tracing techniques and provides a clear structure of ray propagation in dielectrics. There is a problem of angle ambiguity in the solution process, which is studied in detail in [19]. When the individual propagation vectors of the incident, reflected, and transmitted waves been obtain, it is also easy to calculate the reflection and transmission coefficients.

B. FIELD TRACING IN LOSSY MEDIUM

In part A, the propagation vector of the incident, reflecting, and transmitting wave in lossy mediums provide a basic tracing path for the new VSBR method. There is also a need to calculate the field strength transfer of rays. Thurs, the reflection and transmission coefficient is solved as follows:

The Maxwell's equations show as

$$\begin{aligned}\nabla\times\overrightarrow{E} &= -j\omega\mu\overrightarrow{H}\\ \nabla\times\overrightarrow{H} &= j\omega\varepsilon\overrightarrow{E}\end{aligned} \tag{11}$$

which can be expressed by propagation vector $\vec{\gamma}$ as:

$$\overrightarrow{\gamma}\times\overrightarrow{E} = j\omega\mu\overrightarrow{H} \tag{12}$$

$$\overrightarrow{\gamma}\times\overrightarrow{H} = -j\omega\varepsilon\overrightarrow{E} \tag{13}$$

The boundary condition at the interface is defined as:

$$\overrightarrow{n}\times(\overrightarrow{E}_i + \overrightarrow{E}_r) = \overrightarrow{n}\times\overrightarrow{E}_t \tag{14}$$

$$\overrightarrow{n}\times(\overrightarrow{H}_i + \overrightarrow{H}_r) = \overrightarrow{n}\times\overrightarrow{H}_t \tag{15}$$

It is supposed that the incident electric field of vertical polarized wave is $\vec{E}_i = \hat{e}_y E_0 e^{-\vec{\gamma}_i\cdot\vec{r}}$. By applying equation (14) and the equation $\vec{\gamma}_1\cdot\vec{r} = \vec{\gamma}_2\cdot\vec{r}$, the equation (7) is obtained as:

$$E_0 + R_\perp E_0 = T_\perp E_0, \quad 1 + R_\perp = T_\perp \tag{16}$$

where the $R_\perp$ and $T_\perp$ is the reflection and refraction coefficient.

Substituting equations (12) and (15) into equations (16), the $R_\perp$ and $T_\perp$ can be obtained as:

$$\begin{aligned}R_\perp &= \frac{\mu_2(\alpha_1\cos\zeta_1 + j\beta_1\cos\varphi_1) - \mu_1(\alpha_2\cos\zeta_2 + j\beta_2\cos\varphi_2)}{\mu_2(\alpha_1\cos\zeta_1 + j\beta_1\cos\varphi_1) + \mu_1(\alpha_2\cos\zeta_2 + j\beta_2\cos\varphi_2)}\\ T_\perp &= \frac{2\mu_2(\alpha_1\cos\zeta_1 + j\beta_1\cos\varphi_1)}{\mu_2(\alpha_1\cos\zeta_1 + j\beta_1\cos\varphi_1) + \mu_1(\alpha_2\cos\zeta_2 + j\beta_2\cos\varphi_2)}\end{aligned} \tag{17}$$

In addition, if the incident wave is a horizontal polarized wave, the Incident magnetic field is $\overrightarrow{H}_i = \overrightarrow{e}_y H_0 e^{-\overrightarrow{\gamma}_i\cdot\overrightarrow{r}}$. Then the equation (16) can be rewritten as:

$$H_0 + R_\parallel H_0 = T_\parallel H_0, \quad 1 + R_\parallel = T_\parallel \tag{18}$$

Furthermore, the reflection coefficient and the transmission coefficient of the parallel-polarized wave can be obtained as:

$$\begin{aligned}R_\parallel &= \frac{-\varepsilon_2(\alpha_1\cos\zeta_1 + j\beta_1\cos\varphi_1) + \varepsilon_1(\alpha_2\cos\zeta_2 + j\beta_2\cos\varphi_2)}{\varepsilon_2(\alpha_1\cos\zeta_1 + j\beta_1\cos\varphi_1) + \varepsilon_1(\alpha_2\cos\zeta_2 + j\beta_2\cos\varphi_2)}\\ T_\parallel &= \frac{2\varepsilon_2(\alpha_1\cos\zeta_1 + j\beta_1\cos\varphi_1)}{\varepsilon_2(\alpha_1\cos\zeta_1 + j\beta_1\cos\varphi_1) + \varepsilon_1(\alpha_2\cos\zeta_2 + j\beta_2\cos\varphi_2)}\end{aligned} \tag{19}$$

Eventually, the reflection coefficient and transmission coefficient of horizontal and vertical polarized waves of non-uniform plane wave in lossy mediums are solved [20], [22].

C. FAR FIELD SCATTERING INTEGRAL

Far-field scattering of the target is the cumulative contribution of all the field contributions from the ray tube after being reflected by the target surface and after transmission [21]. When the ray is directed at infinity or reaches the threshold number of bounces, the ray tracing is stopped and the far-field scattering field is calculated.

By using the electric field and magnetic field, the equivalent electromagnetic flow density can be calculated. The current density is $\vec{J}_S$, and the magnetic flow density is $\vec{M}_s$.which defined as:

$$\vec{J}_s = \hat{n}\times\vec{H}, \quad \vec{M}_s = -\hat{n}\times\vec{E} \tag{20}$$

When the ray is incident on the surface of the medium from the air, the contributions of the incident field and the reflected field are considered. When the radiation exits the

medium into the air, only the effect of the transmitted field is taken into account. The far-field scattering electric field is obtained by accumulating the fields generated by these equivalent electromagnetic currents as

$$\vec{E}_J^s(\vec{r}) = jk\eta \frac{e^{-jkr}}{4\pi r} \int\int_s \hat{r} \times \hat{r} \times \vec{J}_s(\vec{r}') e^{jk\hat{r}\cdot\vec{r}'} dS'$$
$$\vec{E}_M^s(\vec{r}) = jk \frac{e^{-jkr}}{4\pi r} \int\int_s \hat{r} \times \vec{M}_s(\vec{r}') e^{jk\hat{r}\cdot\vec{r}'} dS' \quad (21)$$

where, η is the wave impedance in free space. $\hat{r}$ is far field scattering field direction. $\vec{r}'$ is the intersection of the ray at the target-air interface.

IV. NUMERICAL RESULTS

This section shows a series of test simulations, starting with simulating simple lossy medium objects, ending with simulating plasma sheath objects. In our simulations, all the computations in this section are carried out on the computer of Intel Xeon E7-4850 CPU equipped with 8GB RAM.

A. LOSSY CUBE TARGET

Firstly, as shown in Fig 3(a), a cube structure of 12 mixed lossy medium sub-blocks with the frequency of 1GHz in the standard atmosphere is analyzed to verify the validity of the proposed method. The entire cube medium consists of twelve small cube mediums. The size and dielectric constant of each small cube is shown in Fig 3 (a). ε_r is the complex dielectric constant and there are 12 cases in total. The permeability μ_r is 1.0. The angles of the incident wave vector are $\theta_i = 45°$, $\varphi_i = 0°$, observation range is $\varphi = 0°$, $\theta = 0° \sim 360°$. It demonstrates the relevance of the new VSBR method. The reference solution is computed with FEKO_FDTD solver. As Fig. 3 (b) shows, in most angles, the result of VSBR method and FEKO_FDTD method can be approximated the same. In this case, the threshold for the number of bounces of the rays is set to 10. Besides, the comparison of computational efficiency between the two methods is given in Table 1. In all the following examples, the error is defined as:

$$error\sigma = \sqrt{\sum \Delta x^2/(n-1)}$$

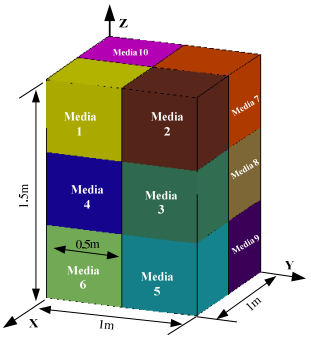

Medium number	dielectric constant
1	(0.68, -0.2)
2	(0.64, -0.2)
3	(0.78, -0.8)
4	(0.82, -1.2)
5	(0.94, -1.8)
6	(0.98, -2.0)
7	(0.60, -0.3)
8	(0.74, -0.6)
9	(0.90, -1.6)
10	(0.56, -0.4)
11	(0.86, -1.4)
12	(0.70, -0.4)

(a)

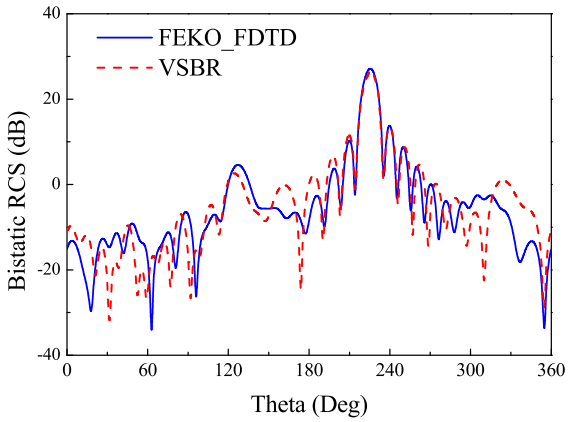

(b)

FIGURE 3. (a) Cube structure of 12 mixed lossy medium sub blocks. (b) Bistatic RCS (VV) of the cube calculated by the FDTD method and the VSBR method.

TABLE 1. The comparison of computational efficiency between the FEKO_FDTD method and VSBR method: The FDTD method and the VSBR method is used on a single CPU core.

	Memory requirement(MB)	CPU time （hour）	Speed up rate
FEKO_FDTD	420	8.00	—
VSBR	86	0.05	160

B. LOSSY CONE TARGET

Then, as shown in Fig 4, we investigate a cone object with 3 cases of layered coated lossy medium surrounding. Dielectric constant are $\varepsilon_r = (0.90, -0.1)$. The size of the object is shown in Fig 4. Meanwhile, as shown in Table 2, the thicknesses of coated mediums for the 3 cases are 0.02meter, 0.05meter and 0.10meter. We calculate the monostatic RCS of the 3 cases objects with the angle $\theta_i = -90° \sim 90°$, $\varphi_i = 0°$. The frequency is 3GHz. We use the FEKO_FDTD method, the traditional triangular meshing method (PO) and the VSBR method to calculate this object. The comparing results of three methods are given in Figs. 5 (a), (b), (c), which corresponds to the condition of

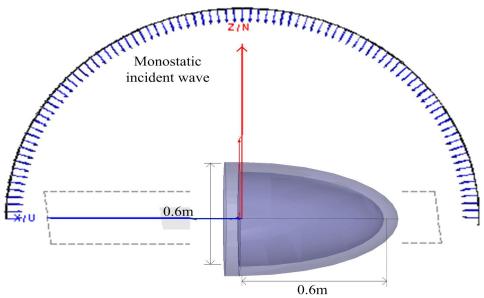

FIGURE 4. Cone structure with coated lossy medium.

TABLE 2. The detailed parameters of coated lossy medium in 3 different conditions.

Thickness of coated medium	Dielectric constant
0.02m (0.2 λ)	$\varepsilon_r = (0.90, -0.1)$
0.05m (0.5 λ)	
0.10m (1.0 λ)	

different thickness of the coated medium. Moreover, we separately give the RCS error of the traditional PO method and VBSR in Fig 5(d), which is compared with FEKO_FDTD method. As shown in Fig. 5 (a), (b), (c), in most angles, the result of VSBR method has good performance compared with FEKO_FDTD method while the traditional (PO) method performed worse. Obviously, as shown in Fig 5(d), with the increase of the thickness, the error of VSBR method is much less than the traditional (PO) method. The FEKO_FDTD method is used as a benchmark. The variation of the error for VSBR is slower while the accuracy of the traditional PO method becomes poor. In this case, the threshold for the number of bounces of the ray is set to 5. Also, for Case 3, the comparison of computational efficiency between the three methods is given in Table 3 as an example.

TABLE 3. The comparison of computational efficiency between the FEKO_FDTD method and VSBR method and the traditional PO mETHED method. All methods are using on a single CPU core.

Case 3	Memory requirement(MB)	CPU time (hour)
FEKO_FDTD	220	2.80
VSBR	26	0.02
The traditional (PO) method	10	0.01

C. PLASMA SHEATH TARGET

Thirdly, to prove the efficiency of VSBR method in calculating the plasma sheath, this example shows the bistatic RCS of a metal warhead at a height of 30 km and a speed of 10 Mach. The radius and length of the Warhead is 0.1m and 0.2m, and the plasma stealth has a radius of 0.4 m and a length of 0.6 m. The Simulating results of the distribution of equivalent permittivity are shown in Fig 6.

We set the frequency of the illuminating radar wave as 3GHz, and the plane wave is incident on the warhead head. The angles of the incident wave vector is $\theta_i = -90°$, $\varphi_i = 0°$,observation range $\varphi = 0°$, $\theta = 0° \sim 360°$ The result of reference solution computed by the FDTD, VSIE and VSBR solver is shown in Fig 7. Besides, the comparison of computational efficiency among three methods is given in Table 4. It is obvious that the VSBR has a highly efficiency. Speed up rate is about 120 in this example. It is worth noting

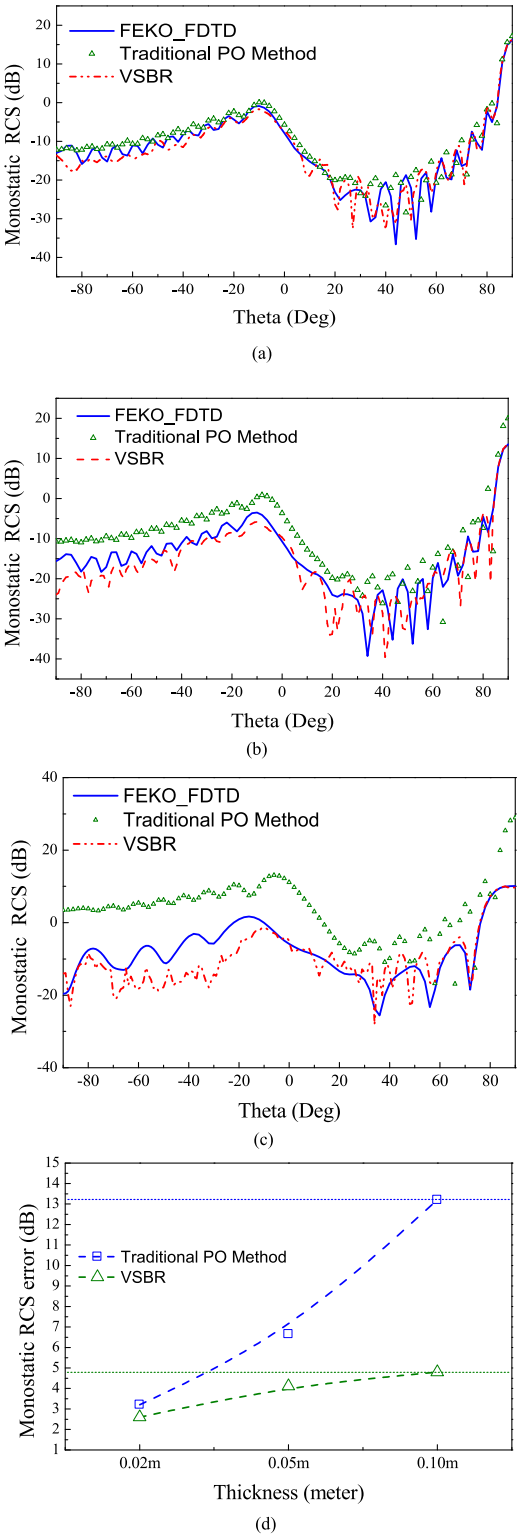

FIGURE 5. Monostatic RCS (VV) for the cone coated with lossy medium by the FDTD method, the VSBR method and the traditional PO method. (a) The thickness of coating is 0.02*m*. (b) The thickness of coating is 0.05*m*. (c) The thickness of coating is 0.10*m*; (d) RCS error of the traditional method (PO) methods and VBSR method with different thicknesses of coating. The error of VSBR method is much less than the traditional (PO) method. The FDTD method is used as a benchmark. As the thickness increases, the variation of the error for the VSBR is slower. The accuracy of the traditional PO method becomes poor.

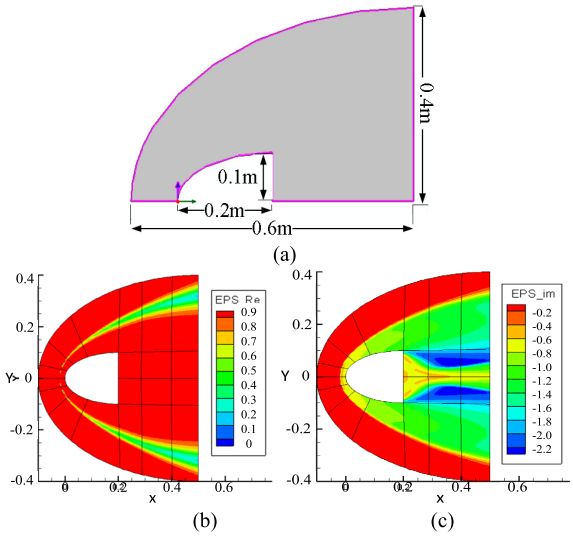

FIGURE 6. (a) Plasma sheath model structure: 2D facet. (b) Real part of dielectric constant. (c) Imaginary part of dielectric constant. The flow field of plasma sheath for the object flying at 10 Mach and 30 km above the ground is calculated by CFD-FANSTRIN. The model is a rotationally periodic structure.

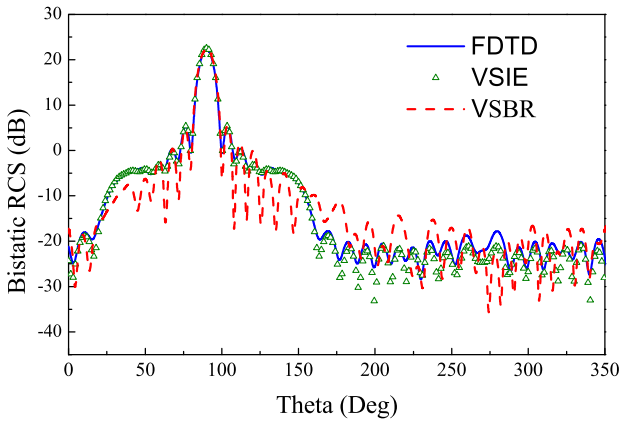

FIGURE 7. Bistatic RCS (VV) for the metal warhead with plasma sheath.

TABLE 4. The comparison of computational efficiency between the FDTD method and VSBR method: The FDTD method VSIE method and the VSBR method is used on a single CPU core.

	Memory requirement(G)	CPU time (hour)
FDTD	30.00	80.00
VSBR	0.48	0.67
VSIE	7.60	102.00

that the VSIE method is also a tetrahedral-mesh method, and the unknowns are the same as the VSBR. In this case, the threshold for the number of bounces of the ray is set to 20. We also calculated the RCS results with a threshold greater than 20 and found that the results have converged.

Simultaneously, we give comparing calculation results by varying mesh sizes. The result is shown in Fig 8 (a). For the 5 cases, the distributions of equivalent permittivity are the same before mapping to each tetrahedral cell. The computing error between the VSBR and the FDTD method is given in Fig 8 (b). As can be seen from Fig. 8 (a) and (b), when the mesh scales are 1/3λ, 1/5λ and 1/6λ, the error is extremely large. When the mesh scale less then 1/8λ. The error is less than 5dB. The FDTD method is used as a benchmark. The unknown amount of 5 different mesh sizes of the plasma sheath and the computation time is given in Table. 5.

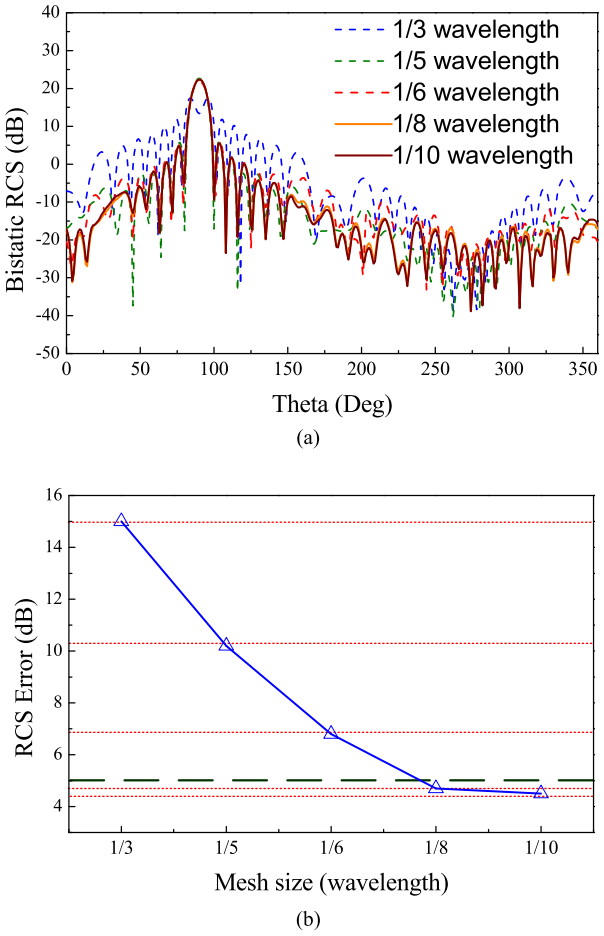

FIGURE 8. (a) Bistatic RCS (VV) for the metal warhead with plasma sheath. (b) RCS error of difference mesh size when comparing with FDTD method.

TABLE 5. The unknown amount of mesh size of the plasma sheath, and the computational time.

Mesh size	Unknowns (number of tetrahedrons)	Threshold of bounces	CPU time (hour)
1/3 λ	61212	15	0.08
1/5 λ	206921	15	0.18
1/6 λ	345223	18	0.20
1/8 λ	1629965	20	0.67
1/10 λ	2201355	22	0.81

Fourthly, another example shows the bistatic RCS of a larger metal warhead at a height of 30 km and a speed of 10 Mach. The radius and length of the Warhead are

0.5m and 3m, and the plasma stealth has a radius of 2 m and a length of 6 m. Simulation results which show the distribution of the flow field and the distribution of equivalent permittivity are shown in Fig.9.

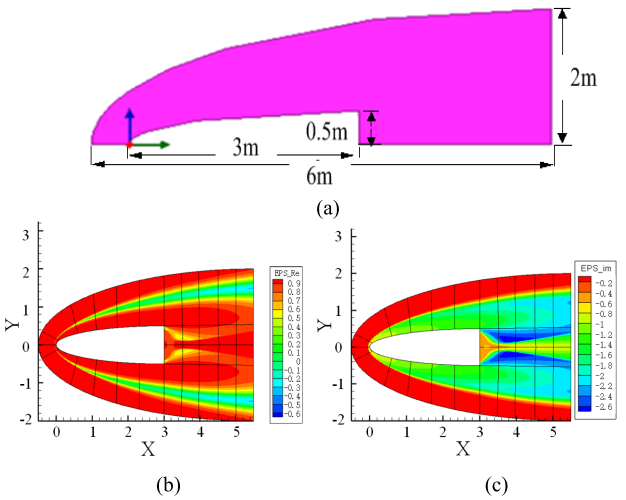

FIGURE 9. **A larger model. (a) Plasma sheath model structure. (b) Real part of dielectric constant. (c) Imaginary part of dielectric constant. The flow field of the plasma sheath for the object flying at 10 Mach and 30 km above the ground is calculated by CFD-FANSTRIN.**

We set the frequency of the illuminating radar wave as 1 GHz, the plane wave is incident on the warhead head. The angles of the incident wave vector is $\theta_i = -45°$, $\varphi_i = 0°$,observation range $\varphi = 0°$, $\theta = 0° \sim 360°$. The result of reference solution in different incident angles calculated by the FDTD and VSBR solver is shown in Fig.10. The calculation time of VSBR method is about 1.8 hours which is much less than the time of FDTD. The unknowns are 11milions. In this case, the threshold for the number of bounces of the ray is set to 30.

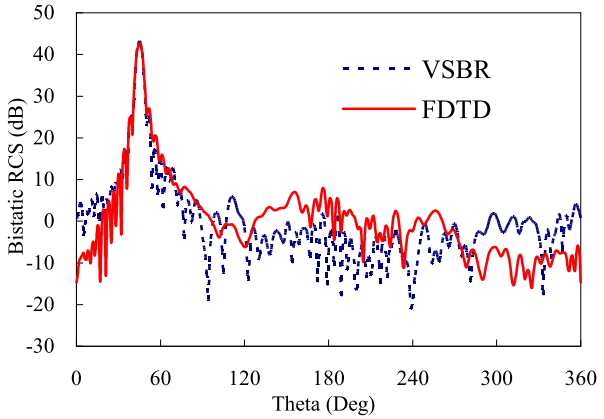

FIGURE 10. **Bistatic RCS (VV) for the larger metal warhead with plasma sheath.**

V. CONCLUSION

The RCS of a hypersonic model cover with inhomogeneous plasma has been studied by the tetrahedron-meshed VSBR method. Firstly, the propagation of electromagnetic waves in the tetrahedral meshed plasma sheath is predicted by the ray tracing method. Then the flow field can be obtained by mapping the permittivity to each tetrahedron cell. At last, the non-uniform plane wave is used to analyze the propagation in the plasma sheath. Compared with the traditional triangle-meshed high-frequency method, the proposed VSBR method can be used as an efficient tool to analyze the plasma sheath with random shapes and varying mediums. Meanwhile, both the time and resource consumption of the proposed VSBR method has a better performance than the FDTD and VSIE methods.

ACKNOWLEDGMENT

The authors would like to thank the efforts and valuable comments from the editors and anonymous reviewers.

REFERENCES

[1] P. E. Bisbing, "Development of a computer model for scattering of electromagnetic waves by a turbulent wake," Re-Entry Environ. Syst. Division, Gen. Electr., Philadelphia, PA, USA, Final Rep., Jun. 1976.
[2] D. J. Gregoire, J. Santoru, and R. W. Schumacher, "Electromagnetic-wave propagation in unmagnetized plasmas," Hughes Res. Labs., Malibu, CA, USA, Final Rep., Jan. 1992.
[3] L.-J. Guo, L.-X. Guo, J.-T. Li, and D. Liu, "Propagation of electromagnetic waves on a relativistically moving non-uniform plasma with WKB method," in *Proc. IEEE Int. Conf. Comput. Electromagn. (ICCEM)*, Guangzhou, China, Feb. 2016, pp. 46–48.
[4] J. Shi, Y. Gao, J. Wang, Z. Yuan, and Y. Ling, "Electromagnetic reflection of conductive plane covered with magnetized inhomogeneous plasma," *Int. J. Infr. Millim. Waves*, vol. 22, no. 8, pp. 1167–1175, Aug. 2001.
[5] Z. Yuan and J. M. Shi, "Collisional, nonuniform plasma sphere scattering calculation by FDTD employing a Drude model," *Int. J. Infr. Millim. Waves*, vol. 28, pp. 987–992, Nov. 2007.
[6] B. Chaudhury and S. Chaturvedi, "Study and optimization of plasma-based radar cross section reduction using three-dimensional computations," *IEEE Trans. Plasma Sci.*, vol. 37, no. 11, pp. 2116–2127, Nov. 2009.
[7] J.-W. Qian, H.-L. Zhang, and M.-Y. Xia, "Modelling of electromagnetic scattering by a hypersonic cone-like body in near space," *Int. J. Antennas Propag.*, vol. 2017, Feb. 2017, Art. no. 3049532.
[8] J. Li, L.-X. Guo, S.-S. Jin, and Q.-J. Fang, "EM wave propagation characteristic in plasma sheath," *Chin. J. Radio Sci.*, vol. 26, no. 3, pp. 494–499, Jun. 2011.
[9] J. W. Qian and M. Y. Xia, "Simulation of scattering by a rotating hypersonic object with plasma sheath," in *Proc. IEEE Int. Conf. Comput. Electromagn.*, Hong Kong, China, Feb. 2015, pp. 258–260.
[10] W. Chen, L. Guo, J. Li, and L. Dan, "Research on the FDTD method of scattering effects oof three dimensional dusty plasma," in *Proc. Int. Appl. Comput. Electromagn. Soc. Symp. (ACES)*, Suzhou, China, Aug. 2017, pp. 1–2.
[11] S.-H. Liu and L.-X. Guo, "Analyzing the electromagnetic scattering characteristics for 3-D inhomogeneous plasma sheath based on PO method," *IEEE Trans. Plasma Sci.*, vol. 44, no. 11, pp. 2838–2843, Nov. 2016.
[12] J. W. Qian, H. L. Zhang, and M. Y. Xia, "Backscattering of a hypersonic cone with plasma sheath at different attack angles," in *Proc. IEEE Int. Conf. Comput. Electromagn. (ICCEM)*, Guangzhou, China, Feb. 2016, pp. 1–3.
[13] M. P. Bachynski, T. W. Johnston, and I. P. Shkarofsky, "Electromagnetic properties of high-temperature air," *Proc. IRE*, vol. 48, no. 3, pp. 347–356, Mar. 1960.
[14] J. D. Anderson, *Hypersonic and High Temperature Gas Dynamics*, 2nd ed. Reston, VA, USA: AIAA, 2006, pp. 375–395.
[15] R. Brem and T. F. Eibert, "A shooting and bouncing ray (SBR) modeling framework involving dielectrics and perfect conductors," *IEEE Trans. Antennas Propag.*, vol. 63, no. 8, pp. 3599–3609, Aug. 2015.
[16] R. B. Adler, "Electromagnetic energy transmission and radiation," *Students Quart. J.*, vol. 31, no. 122, pp. 123–124, Dec. 1960.
[17] R. D. Radcliff and C. A. Balanis, "Modified propagation constants for nonuniform plane wave transmission through conducting media," *IEEE Trans. Geosci. Remote Sens.*, vol. GRS-20, no. 3, pp. 408–411, Jul. 1982.

[18] J. E. Roy, "New results for the effective propagation constants of nonuniform plane waves at the planar interface of two lossy media," *IEEE Trans. Antennas Propag.*, vol. 51, no. 6, pp. 1206–1215, Jun. 2003.
[19] F. Frezz and N. Tedeschi, "On the electromagnetic power transmission between two lossy media: Discussion," *J. Opt. Soc. Amer. A, Opt. Image Sci.*, vol. 29, no. 11, pp. 2281–2288, Nov. 2012.
[20] M. M. Hussnain and M. J. Mughal, "Uniform plane wave reflection from PEC plane embedded in a nonlinear medium," *Prog. Electromagn. Res. M*, vol. 18, pp. 31–42, 2011.
[21] H. Ling, R.-C. Chou, and S.-W. Lee, "Shooting and bouncing rays: Calculating the RCS of an arbitrarily shaped cavity," *IEEE Trans. Antennas Propag.*, vol. 37, no. 2, pp. 194–205, Feb. 1989.
[22] H. Kim and H. Ling, "Electromagnetic scattering from an inhomogeneous object by ray tracing," *IEEE Trans. Antennas Propag.*, vol. 40, no. 5, pp. 517–525, May 1992.

ZHOU CONG was born in Jiangsu, China. He received the B.Sc. degree in detection guidance and control technology from the School of Electrical Engineering and Optical Technique, Zijing College, Nanjing University of Science and Technology, Nanjing, China, in 2013, and the master's degree from the University of Nottingham, from 2015 to 2016, U.K. He is currently pursuing the Ph.D. degree with the Nanjing University of Science and Technology.

His research interests include computational electromagnetics, antenna, and RF-integrated circuits.

ZI HE was born in Hebei, China. She received the B.Sc. and Ph.D. degrees in electronic information engineering from the School of Electrical Engineering and Optical Technique, Nanjing University of Science and Technology, Nanjing, China, in 2011 and 2016, respectively. She was a Visiting Scholar with the University of Illinois at Urbana and Champaign (UIUC), from 2015 to 2016. She holds a postdoctoral position at the Science and Technology on Electromagnetic Scattering Laboratory, BIEF.

Since 2016, she has been an Assistant Professor with the Department of Communication Engineering, Nanjing University of Science and Technology. Her research interests include antenna, RF-integrated circuits, and computational electromagnetics.

RUSHAN CHEN (M'01–SM'15) was born in Jiangsu, China. He received the B.Sc. and M.Sc. degrees from the Department of Radio Engineering, Southeast University, China, in 1987 and 1990, respectively, and the Ph.D. degree from the Department of Electronic Engineering, City University of Hong Kong, in 2001.

He joined the Department of Electrical Engineering, Nanjing University of Science and Technology (NJUST), China, where he became a Teaching Assistant, in 1990, and a Lecturer, in 1992. Since 1996, he has been a Visiting Scholar with the Department of Electronic Engineering, City University of Hong Kong, first as a Research Associate, then as a Senior Research Associate, in 1997, a Research Fellow, in 1998, and a Senior Research Fellow, in 1999. In 1999, he was also a Visiting Scholar with Montreal University, Canada. In 1999, he was promoted to Full Professor and Associate Director of the Microwave and Communication Research Center, NJUST, where he was appointed as the Head of the Department of Communication Engineering, in 2007. He was appointed as the Dean of the School of Communication and Information Engineering, Nanjing University of Posts and Telecommunications, in 2009. And in 2011, he was appointed as the Vice Dean of the School of Electrical Engineering and Optical Technique, NJUST. He has authored or coauthored more than 200 papers, including over 140 papers in international journals. His research interests mainly include microwave/millimeter-wave systems, measurements, antenna, RF-integrated circuits, and computational electromagnetics.

Dr. Chen was selected as a member of the Electronic Science and Technology Group by the Academic Degree Commission of the State Council, in 2009. He is a Senior Member of the Chinese Institute of Electronics (CIE) and the Vice President of the Microwave Society of CIE and the IEEE MTT/APS/EMC Nanjing Chapter. He received the 1992 Third-Class Science and Technology Advance Prize given by the National Military Industry Department of China, the 1993 Third-Class Science and Technology Advance Prize given by the National Education Committee of China, the 1996 Second-Class Science and Technology Advance Prize given by the National Education Committee of China, the 1999 First-Class Science and Technology Advance Prize given by Jiangsu Province, and the 2001 Second-Class Science and Technology Advance Prize. He was a recipient of the Foundation for China Distinguished Young Investigator Award presented by the National Science Foundation (NSF) of China, in 2003. In 2008, he became a Chang-Jiang Professor under the Cheung Kong Scholar Program awarded by the Ministry of Education, China. He serves as a Reviewer for many technical journals, such as the IEEE TRANSACTIONS ON ANTENNAS AND PROPAGATION, the IEEE TRANSACTIONS ON MICROWAVE THEORY AND TECHNIQUES, and *Chinese Physics*, and now serves as an Associate Editor for the *International Journal of Electronics*.